Supporting Information

Reducing Exciton Binding Energy of Antimony-based Perovskite via Improving Phase Purity for Efficient Solar Cells

Tengyu Xu,[a] Xian Zhang,[a] Fangzhou Liu,*[a] Huichao Guo,[a] Jiaqi Zhang,[a] Shaogeng Cai,[a] Deao Li,[a] Yangyang Zhang,[a] Yan Guan,*[b] Wenjin Yu,[c] Dechun Zou,[b] Lixin Xiao,*[c] and Cuncun Wu*[a]

a. Tianjin Key Laboratory of Materials Laminating Fabrication and Interface Control Technology, School of Materials Science and Engineering, Hebei University of Technology, Tianjin 300401, P. R. China.

b. College of Chemistry and Molecular Engineering, Peking University, Beijing 100871, P. R. China.

c. State Key Laboratory for Artificial Microstructure and Mesoscopic Physics, Department of Physics, Peking University, Beijing 100871, P. R. China.

E-mail: liufz@hebut.edu.cn; yanguan@pku.edu.cn; lxxiao@pku.edu.cn; cuncunwu@hebut.edu.cn

Experimental Section

Materials: FTO-coated glass substrates, Spiro-OMeTAD (99.86%), 4-*tert*-butylpyridine (Tbp,99%), lithium-bis-(trifluoromethanesulfonyl) imide (Li-TFSI, 99%), and acetonitrile (99.9%) were purchased Advanced Election Technology Co. Ltd. Methylammonium chloride (MACl, 99.5%) and cesium iodide (CsI, 99.5%) were purchased from Xi'an Polymer Light Technology Corp., China. Chlorobenzene (CB, 99.99%) and dimethyl sulfoxide (DMSO, 99.7%) were purchased from J&K Scientific. Titanium tetrachloride ($TiCl_4$, 99.9%) was purchased from Aladdin Reagent Shanghai Co. Ltd. Antimony (III) iodide (SbI_3, 99.999%) was purchased from Beijing InnoChem Science & Technology Co. Ltd. All of these commercially available materials were used as received without any further purification.

Solar Cell Fabrication: The FTO-coated glass substrates were cleaned ultrasonically in detergent, deionized water, and ethanol. The cleaned FTO-coated glass substrates were then dried with nitrogen. After drying, the substrates were further treated with UV-ozone for 15 min. TiO_2 thin layer was prepared following a chemical bath deposition method.[1] Briefly, the cleaned FTO substrates were immersed in an aqueous $TiCl_4$ solution (4 ml of $TiCl_4$ in 200 ml of DI water) and then dried at 70 °C for 1.5 h. The substrates with TiO_2 layer were thoroughly washed with DI water and dried at 150 °C for 60 mins in ambient before use. Perovskite precursor solutions were prepared by dissolving CsI and SbI_3 with a molar ratio of 3:2, 3:2.2, 3:2.3, and 3:2.4, respectively, in 1 ml of DMSO with the addition of 40 mg of MACl. All the precursor

solutions share a Cs^+ concentration of 1.2 M. The perovskite precursor solution was then deposited via spin coating onto the TiO_2 layer at 3000 rpm for 15 s, followed by low pressure-assisted treatment for 60 s and annealing at 150 °C for 10 min. For the hole transport layer, a precursor solution was prepared by dissolving 72.3 mg of spiro-OMeTAD, 28.8 μL of tBP, and 17.5 μL of pre-dissolved Li-TFSI solution (520 mg of Li-TFSI in 1 mL of acetonitrile) in 1 ml of chlorobenzene. The precursor solution was then spin-cast onto the perovskite films at 4000 rpm for 30 s. Finally, 50 nm of gold was thermally evaporated atop the hole transport layer through a shadow mask as the electrode. The Sb-based PSC devices were completed with an n-i-p configuration of FTO/TiO_2/$Cs_3Sb_2Cl_xI_{9-x}$/spiro-OMeTAD/Au and an active area of 0.1 cm^2.

Film and Device Characterizations: For film characterizations, SEM images of the perovskite films prepared on TiO_2-coated glass/FTO substrates were obtained using a JEOL JSM-7610F scanning electron microscope. XRD analysis of the perovskite films were performed using a Rigaku SmartLab X-ray diffractometer with Cu Kα radiation. UV-vis absorption spectra were collected using a Shimadzu UV-1900 spectrophotometer in the wavelength range from 300 nm to 900 nm. GIWAXS measurements were performed using Xenocs Xeuss 2.0 (GI-)SAXS/WAXS/USAXS beamline system with the wavelength of the incident X-ray beam of 0.154 nm. The GIWAXS patterns were collected by a Pilatus 300 K detector with the sample-to-detector distance of 150 mm, and calibrated by the silver behenate standard sample. Atomic force microscopy (AFM) and conductive atomic force microscopy (C-AFM) studies were performed using Asylum Research MFP 3D Atomic Force Microscope. For C-AFM test, a bias voltage of +1 V was applied between the conductive probe and the sample surface. Temperature dependent PL spectra from 80 K to 300 K were measured using a NanoLog spectrofluorometer in the wavelength range of 490-900 nm with a 450 nm excitation source. Dielectric measurements of the films were performed in the dark with parallel-plate capacitor devices of ITO /perovskite/Au using CHI660E electrochemical workstation.

For device characterizations, dark and light *J-V* curves of the devices were measured using a Keithley 2400 sourcemeter. To assess the photovoltaic performance, Sb-based PSC devices were subjected to AM 1.5G simulated solar irradiation (EASISOLAP-50-3A solar simulator, CROWNTECH, INC) at 100 mW cm^{-2}. The light intensity of the solar simulator was calibrated using a certified reference cell. The IPCE spectra was recorded using an Enli Technology EQE measurement system (QE-R) and the light intensity at each wavelength was calibrated with a standard single crystal Si photovoltaic cell. Mott-Schottky measurement were performed by CHI660E electrochemical workstation at a frequency of 1 kHz. Electrochemical impedance

spectroscopy (EIS) was measured by applying a bias of the open-circuit voltage with an CHI660E electrochemical workstation under dark conditions. The scanning frequency was set between 1 Hz and 10^5 Hz. All device characterizations were performed in ambient without encapsulation.

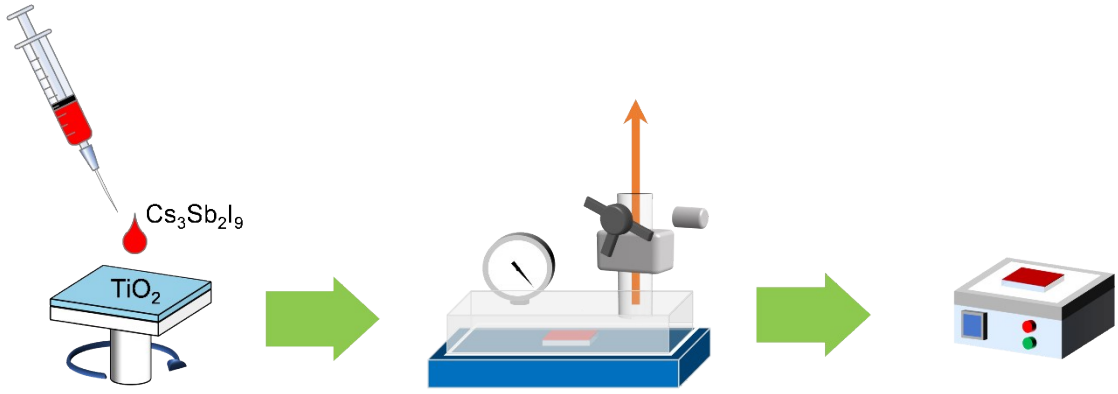

Figure S1. Schematic of low pressure assisted (LPA) synthesis of antimony-based perovskite films.

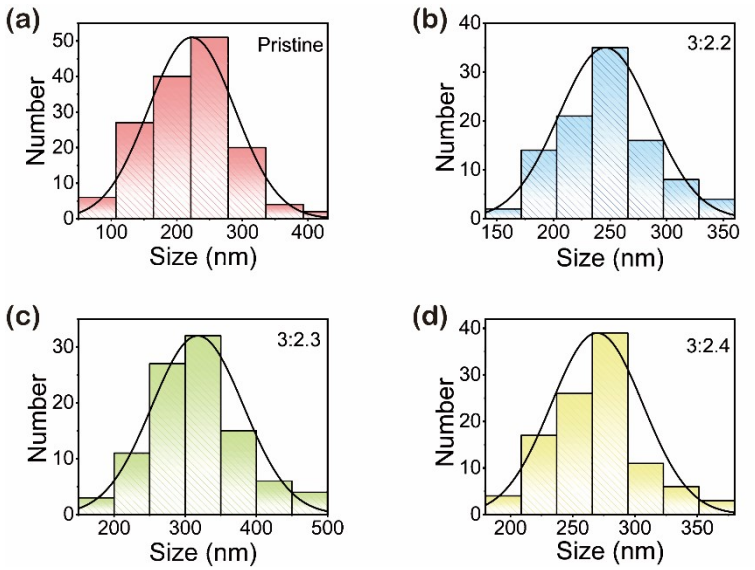

Figure S2. Histograms of grain sizes for the $Cs_3Sb_2Cl_xI_{9-x}$ films with various precursor SbI_3 contents.

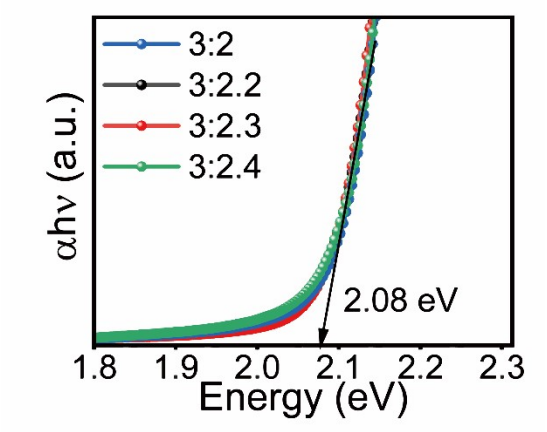

Figure S3. Tauc plots of the absorption spectra for the $Cs_3Sb_2Cl_xI_{9-x}$ films with various precursor SbI_3 contents.

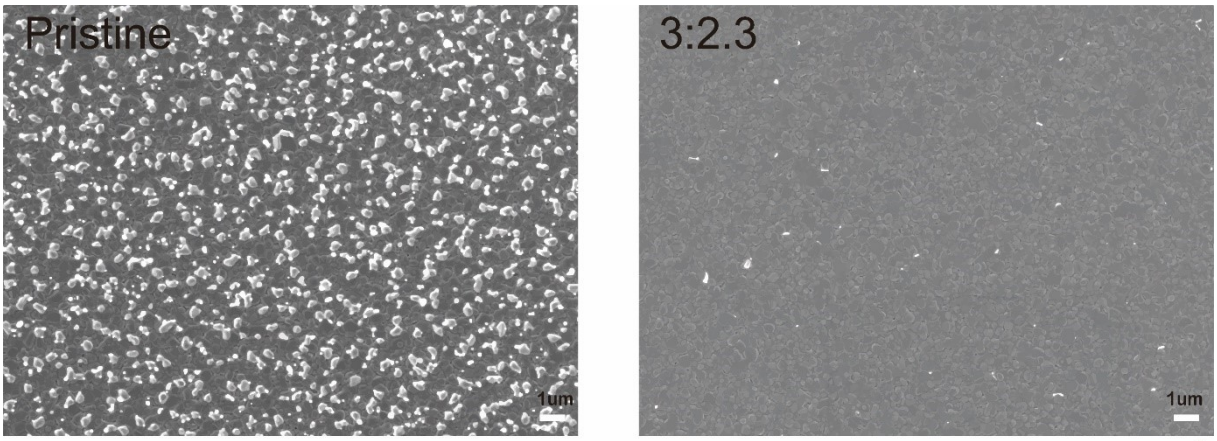

Figure S4. Low magnification SEM images of the Pristine film and the 3:2.3 film.

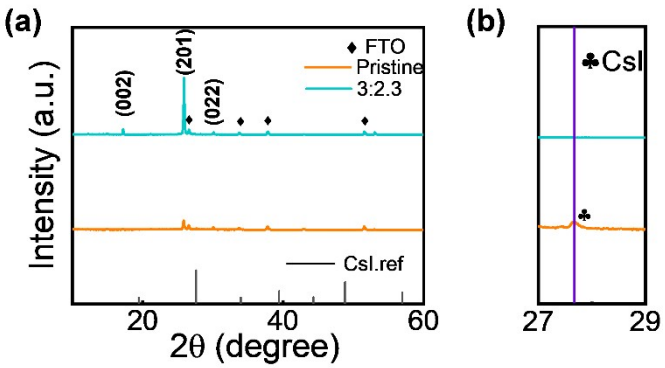

Figure S5. a) XRD patterns of the Pristine and 3:2.3 samples, and b) the corresponding zoomed view in the 2θ range of 27-29°.

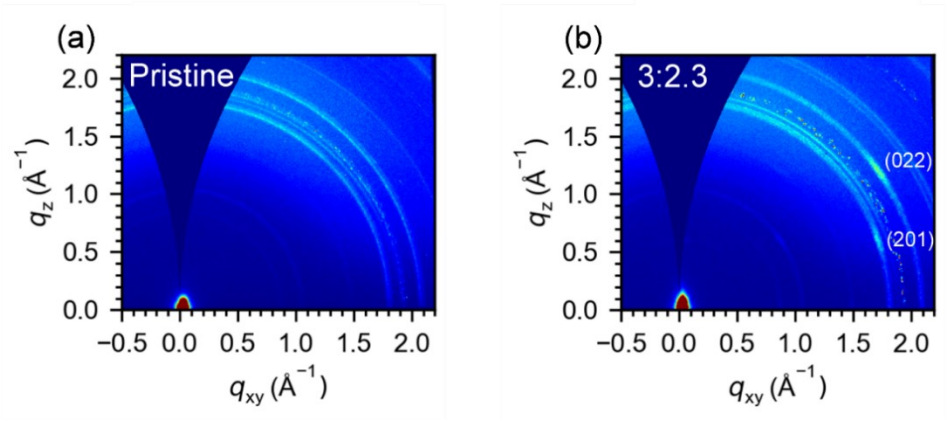

Figure S6. GIWAXS patterns of the Pristine sample and the 3:2.3 sample.

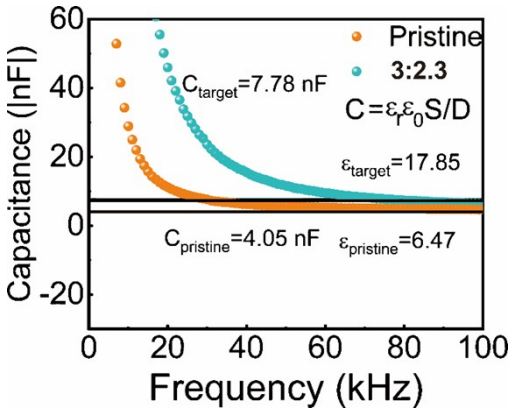

Figure S7. Capacitance as a function of frequency obtained with parallel-plate capacitor devices and the calculated relative dielectric constant for the Pristine and 3:2.3 samples.

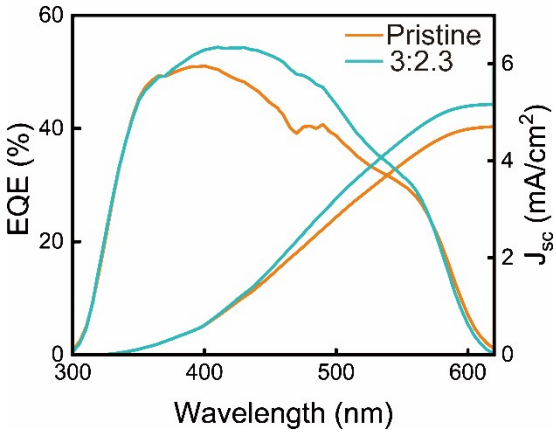

Figure S8. EQE spectra of the Pristine device and the 3:2.3 device.

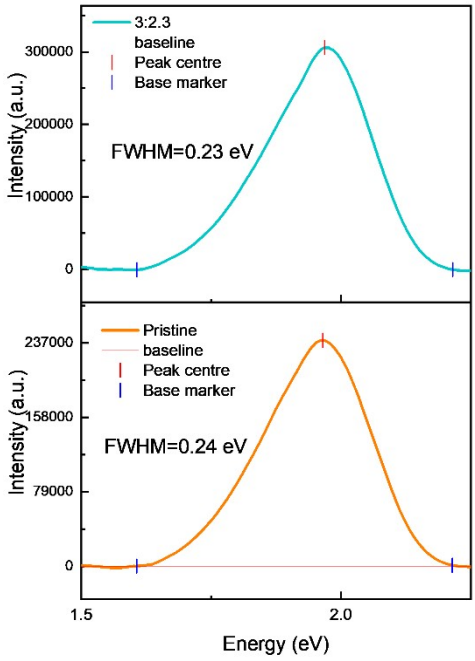

Figure S9. PL spectra of the Pristine sample and the 3:2.3 sample at 300 K.

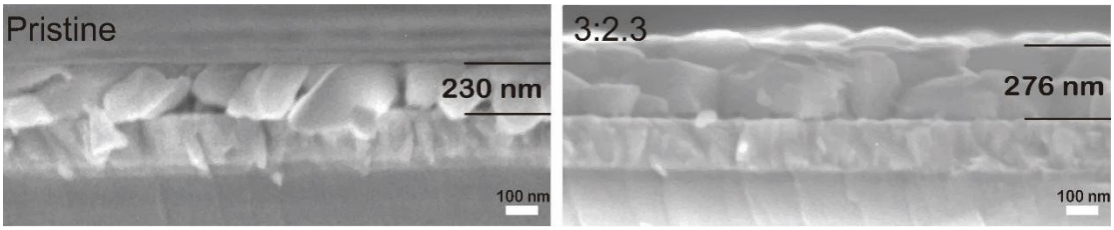

Figure S10. Cross-sectional SEM image of the Pristine sample and the 3:2.3 sample.

Table S1. The photovoltaic parameters of 15 individual PSC devices for the Pristine devices and the 3:2.3 devices.

Device Type	Sample No.	J_{sc} (mA/cm^2)	V_{oc} (V)	FF (%)	PCE (%)
Pristine	1	4.88	0.803	65	2.55
	2	4.86	0.819	63	2.51
	3	5.14	0.764	62	2.43
	4	5.16	0.773	62	2.47
	5	5.47	0.778	65	2.76
	6	5.23	0.792	63	2.61
	7	5.34	0.804	64	2.74
	8	5.44	0.786	63	2.70
	9	5.52	0.809	56	2.50
	10	5.85	0.811	64	3.04

	11	5.38	0.793	60	2.56
	12	6.11	0.796	52	2.53
	13	6.44	0.776	50	2.58
	14	5.46	0.781	66	2.81
	15	6.04	0.788	58	2.76
	average	5.488	0.792	60.8	2.64
3:2.3	1	6.21	0.809	66	3.32
	2	5.57	0.806	71	3.19
	3	5.11	0.807	72	2.97
	4	6.27	0.813	67	3.42
	5	5.09	0.802	70	2.86
	6	5.4	0.82	68	3.01
	7	5.36	0.822	68	2.99
	8	5.59	0.827	72	3.33
	9	5.41	0.833	68	3.06
	10	5.82	0.805	70	3.28
	11	6.01	0.815	66	3.23
	12	5.96	0.805	67	3.21
	13	5.86	0.806	62	2.93
	14	5.81	0.800	66	3.07
	15	5.68	0.814	63	2.91
	average	5.68	0.812	67.7	3.12

Table S2. A summary of the PCE for all inorganic Sb-based PSCs with the n-i-p architecture reported in literature and in this work.

Active Layer	Structure	PCE (%)	Year	Ref.
$Cs_3Sb_2I_9$(0D)	FTO/c-TiO_2/ $Cs_3Sb_2I_9$(0D)/PTAA/Au	≈0.06	2015	2
$Cs_3Sb_2I_9$(2D)	FTO/TiO_2/ $Cs_3Sb_2I_9$(2D)/Au	1.21	2019	3
$Cs_3Sb_2Cl_xI_{9-x}$	FTO/c-TiO_2/m-TiO_2/ $Cs_3Sb_2Cl_xI_{9-x}$/poly-TPD/Au	2.15	2020	4
$Rb_{0.15}Cs_{2.85}Sb_2Cl_xI_{9-x}$	FTO/Nb_2O_5/ $Rb_{0.15}Cs_{2.85}Sb_2Cl_xI_{9-x}$/P3HT/C	2.46	2021	5
$Cs_3Sb_2Cl_xI_{9-x}$	FTO/TiO_2/ $Cs_3Sb_2Cl_xI_{9-}$	2.5	2022	6

	$_x$/P3HT/Au			
$Cs_3Sb_2Cl_xI_{9-x}$	FTO/c-TiO_2/$Cs_3Sb_2Cl_xI_{9-x}$/spiro-OMeTAD/Au	3.2	2023	[7]
$Cs_3Sb_{2.3}Cl_xI_{9-x}$	FTO/c-TiO_2/$Cs_3Sb_2Cl_xI_{9-x}$/spiro-OMeTAD/Au	3.42	2024	Our work

Table S3. The Urbach energy of the $Cs_3Sb_2Cl_xI_{9-x}$ with various precursor SbI_3 contents

Sample	slope	Urbach energy (meV)
Pristine	10.87	92
3:2.2	10.69	93
3:2.3	12.08	82
3:2.4	10.32	96

Table S4. The FWHM changes of Pristine and 3:2.3 samples at different temperatures

Temperature	Pristine	3:2.3
80 K	0.20809	0.20345
90 K	0.20638	0.20409
100 K	0.20799	0.20311
110 K	0.20809	0.20261
120 K	0.20809	0.20235
130 K	0.21398	0.20334
140 K	0.22178	0.21156
150 K	0.23793	0.22132
160 K	0.25992	0.23615
170 K	0.28589	0.24116
180 K	0.33379	0.25404
190 K	0.34951	0.25526
200 K	0.39366	0.25028

References

1. X. Zhang, Y. Guan, Y. Zhang, W. Yu, C. Wu, J. Han, Y. Zhang, C. Chen, S. Zheng and L. Xiao, *Adv. Opt. Mater.*, 2022, **10**, 202201598.
2. B. Saparov, F. Hong, J.-P. Sun, H.-S. Duan, W. Meng, S. Cameron, I. G. Hill, Y. Yan and D. B. Mitzi, *Chem. Mater.*, 2015, **27**, 5622-5632.
3. F. Umar, J. Zhang, Z. Jin, I. Muhammad, X. Yang, H. Deng, K. Jahangeer, Q. Hu, H. Song and J. Tang, *Adv. Opt. Mater.*, 2019, **7**, 201801368.
4. Y. Peng, F. Li, Y. Wang, Y. Li, R. L. Z. Hoye, L. Feng, K. Xia and V. Pecunia, *Appl. Mater. Today*, 2020, **19**, 100637.
5. Y. Guo, J. Zhou, F. Zhao, Y. Wu, J. Tao, S. Zuo, J. Jiang, Z. Hu and J. Chu, *Nano Energy*, 2021, **88**, 106281.
6. A. Hiltunen, N. Lamminen, H. Salonen, M. Liu and P. Vivo, *Sustain. Energy Fuels*, 2022, **6**, 217-222.

7. Y. Zhang, F. Liu, H. Su, W. Yu, Y. Zou, C. Wu, X. Zhang, J. Zhang, Y. Liang, J. Han, Y. Guan, Y. Zhang, Z. Ye, R. Li, L. Xiao and S. Zheng, *Adv. Funct. Mater.*, 2023, **33**, 202304063.